XXI IMEKO World Congress "Measurement in Research and Industry"
August 30 - September 4, 2015, Prague, Czech Republic

ANALYSIS OF END-SHORTING EFFECT ON ELECTROMAGNETIC FLOWMETER

Satoshi Honda

Affiliation (Faculty of Science & Technology, Keio University), Yokohama, Japan, honda@appi.keio.ac.jp

Abstract - This study analyzes an end-shorting effect on electromagnetic flowmeters with short distance between connecting flanges around about 5D or more. The Bevir's formulation is extended to a conducting pipe wall. Through the evaluation of the Green function satisfying the corresponding boundary conditions, the author's previous formula is reviced.

Keywords: electromagnetic flowmeter, end-shorting effect

1. INTRODUCTION

Electro-magnetic flowmeters have been one of the standard meters to measure liquid flowrate in industry. Theoretical background has been confirmed in the literatures; standard exhaustive text books were written by Shercliff[1] and Schmmartz[2].

Conventional electromagnetic flowmeters have almost uniform magnetic field, and a pair of point electrodes is installed on a circular pipe, where output flow signal is proportional to the flowrate when the velocity profile is axisymmetric. To increse the SNR, almost all conventional and commercially available flowmeters adopt low frequency rectangular wave and additional higher frequency waves to drive the field with well designed coils. Due to the progress in designing the driving coil, magnetic flowmeters have been reduced in length down to 5D; since finiteness of the meter turns out the dependence of the flow signal on liquid conductivities, a compensation method was implemented[3].

After the introduction of the weight vector by Bevir[4], characteristics of the electromagnetic flowmeters were analysed rigourously through this concept for the various setups including variations of driving magnetic fields[5], [6], [7] and meter size finiteness[8].

This paper describes an additional strict treatment of the effect of the connected pipelines of a conductive wall, which brings the dependency on liquid conductivity for the meters of short meter lengths. The author has been extended the Bevir's weight vector to analyze the finiteness of the meter[9], and this paper describes more accurate formula.

2. THEORETICAL BACKGROUND

The electro-magnetic flowmeter has a long history from Faraday, and the theoretical basis have been founded in literatures. We extend the formulation by Bevir[4] to the flowmeter of finite length. The formulation and the weight vectors were already been extended to include displacement current $\partial \boldsymbol{D}/\partial t$ to treat the high frequency field[10],[11]. Operational principle of electromagnetic flowmeters are given by Maxwell's equations, providing that permeability of the fluid is equal to μ_o of vacuum and flow velocity is much smaller than the speed of light. The condition for immediate dielectric relaxation[1],[12], that is negligible displacement current, is $\omega\epsilon/\sigma \ll 1$, where ω denotes field excitation angular frequency, ϵ, electrical permiability, and σ, electrical conductivity.

In order to extend Bevir's formulation[4] to include the vector potential $\boldsymbol{A}$ and displacement current, let U, $\boldsymbol{j}$ and $\boldsymbol{D}$ be potential and current and electric flux densities when driving unit alternating current $e^{-\mathrm{i}\omega t}$ is fed between the electrodes S_1 and S_2 without the fluid motion and field excitation; let U^{m}, $\boldsymbol{j}^{\mathrm{m}}$ and $\boldsymbol{D}^{\mathrm{m}}$ be the potential and current and electrical densities induced by the fluid motion under the field excitation.

$$\boldsymbol{j} = \sigma\boldsymbol{E} = -\sigma \operatorname{grad} U, \tag{1}$$

$$\boldsymbol{D} = \epsilon\boldsymbol{E} = -\epsilon \operatorname{grad} U, \tag{2}$$

$$\begin{aligned}\boldsymbol{j}^{\mathrm{m}} &= \sigma(\boldsymbol{E}^{\mathrm{m}} + \boldsymbol{v}\times\boldsymbol{B}) \\ &= \sigma\left(-\operatorname{grad} U^{\mathrm{m}} - \frac{\partial \boldsymbol{A}}{\partial t} + \boldsymbol{v}\times\boldsymbol{B}\right),\end{aligned} \tag{3}$$

$$\begin{aligned}\boldsymbol{D}^{\mathrm{m}} &= \epsilon\boldsymbol{E}^{\mathrm{m}} + (\epsilon-\epsilon_o)\boldsymbol{v}\times\boldsymbol{B} \\ &= \epsilon\left(-\operatorname{grad} U^{\mathrm{m}} - \frac{\partial \boldsymbol{A}}{\partial t}\right) + (\epsilon-\epsilon_o)\boldsymbol{v}\times\boldsymbol{B}.\end{aligned} \tag{4}$$

With these notations, we follow and revice the Bevir's formulation and obtain the flow signal by the following surface integral description:

$$\begin{aligned}U_o &= \iint_S \left[U^{\mathrm{m}}\left(\boldsymbol{j} + \frac{\partial \boldsymbol{D}}{\partial t}\right) - U\left(\boldsymbol{j}^{\mathrm{m}} + \frac{\partial \boldsymbol{D}^{\mathrm{m}}}{\partial t}\right)\right]\cdot d\boldsymbol{S} \\ &= (U_1 - U_2)e^{-\mathrm{i}\omega t}.\end{aligned} \tag{5}$$

By using Gauss integral formula, it is converted to the volume integral,

$$\begin{aligned}U_o = \iiint_V \Bigg[&(\operatorname{grad} U^{\mathrm{m}})\cdot\left(\boldsymbol{j} + \frac{\partial \boldsymbol{D}}{\partial t}\right) \\ &-(\operatorname{grad} U)\cdot\left(\boldsymbol{j}^{\mathrm{m}} + \frac{\partial \boldsymbol{D}^{\mathrm{m}}}{\partial t}\right)\Bigg]\, d\tau,\end{aligned} \tag{6}$$

where vector identity $\operatorname{div}\operatorname{rot} \equiv 0$ is applied to give $\operatorname{div}\operatorname{rot}\boldsymbol{H} = \operatorname{div}(\boldsymbol{j} + \partial\boldsymbol{D}/\partial t) = 0$. If we take the

same frequency ω for driving magnetic flux density $\boldsymbol{B}$ and virtual current density $\boldsymbol{j}$, all field variables have the time dependence $e^{-\mathrm{i}\omega t}$, and partial derivative with respect to time t can be replaced by $-\mathrm{i}\omega$. Substituting the equations (4),..., and (7) in the above volume integral, and some manipulations give the output signals between electrodes in the following separated formulas:

$$U_o = U_\mathrm{A} + U_\mathrm{v}, \tag{7}$$

$$U_\mathrm{A} = -\iiint_V \left(\boldsymbol{j} + \frac{\partial \boldsymbol{D}}{\partial t}\right) \cdot \frac{\partial \boldsymbol{A}}{\partial t}\, d\tau, \tag{8}$$

$$U_\mathrm{v} = \frac{\sigma - \mathrm{i}\omega(\epsilon - \epsilon_o)}{\sigma - \mathrm{i}\omega\epsilon} \iiint_V \left(\boldsymbol{j} + \frac{\partial \boldsymbol{D}}{\partial t}\right) \cdot (\boldsymbol{v} \times \boldsymbol{B})\, d\tau. \tag{9}$$

The signal, U_A, depends on eddy currents induced by vector potential of the driving field, and U_v, on flow velocity field. The latter component coincides the output flow signal of the conventional electromagnetic flowmeter[12].

If the fluid has enough conductivity and displacement current can be ignored as in usual operation, the flowmeter signals are reduced to,

$$U_\mathrm{A} = -\iiint_V \boldsymbol{j} \cdot \frac{\partial \boldsymbol{A}}{\partial t}\, d\tau, \tag{10}$$

$$U_\mathrm{v} = \iiint_V \boldsymbol{j} \cdot (\boldsymbol{v} \times \boldsymbol{B})\, d\tau = \iiint_V (\boldsymbol{B} \times \boldsymbol{j}) \cdot \boldsymbol{v}\, d\tau. \tag{11}$$

Conventional electromagnetic flowmeters have been designed to cancel the first component U_A by using the symmetric configuration of driving coils and electrodes. We have proposed the use of the eddy current dependent component for auto calibration[10].

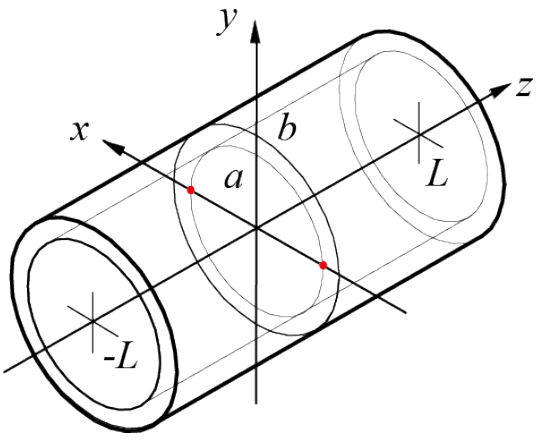

Fig. 1. Flow channel and coordinate system.

3. POTENTIAL UNDER END-SHORTING PHENOMENA

Let us consider the short electromagnetic flowmeter with the length of $2L$ and the pipe inside diameter of $D = 2a$ inserted in the pipeline with a sufficiently conductive wall. Figure 1 shows the flow channel and the coordinate system. Since we have distinct regions as the flowmeter, $|z| \le L$, and the pipelines, $|z| > L$, the Bevir's original formulation cannot be applied directly. Hence, we adopt Green's theorem which is equivalent to the Bevir's formulation.

When the displacement current can be ignored, static electrical scalar potential ϕ describes meter characteristics, which has been obtained by solving the following potential problem in the cylindrical coordinates:

$$\Delta\phi_0(\boldsymbol{x}) = \mathrm{div}\,(\boldsymbol{v} \times \boldsymbol{B}), \tag{12}$$

$$\left.\frac{\partial \phi}{\partial \rho}\right|_{\rho=a} = 0, \qquad |z| \le L, \tag{13}$$

$$\phi_0(a, \varphi, z) = 0, \qquad |z| > L, \tag{14}$$

where insulating liner of the meter and pipe line grounding are assumed. This problem is solved through the solution of the Green function $G_0(\boldsymbol{x}; \boldsymbol{x}_0)$ for the following corresponging problem:

$$\Delta G_0(\boldsymbol{x}; \boldsymbol{x}_0) = -\,\delta(\boldsymbol{x} - \boldsymbol{x}_0), \tag{15}$$

$$\left.\frac{\partial G_0}{\partial \rho_0}\right|_{\rho_0=a} = 0, \qquad |z_0| \le L, \tag{16}$$

$$G_0|_{\rho_0=a} = 0, \qquad |z_0| > L. \tag{17}$$

An exact form of this Green function in the cylindrical coordinates reads

$$\begin{aligned} G_0(\boldsymbol{x}; \boldsymbol{x}_0) = \sum_{m=0}^{\infty} \frac{\epsilon_m}{2\pi^2} \cos\, m(\varphi - \varphi_0) \\ \cdot \int_0^\infty \left[K_m(\lambda\rho_0) - \frac{K_m'(\lambda a)}{I_m'(\lambda a)} I_m(\lambda\rho_0)\right] \\ \cdot I_m(\lambda\rho) \cos\lambda(z - z_0)\, d\lambda, \qquad |z_0| \le L, \end{aligned} \tag{18}$$

$$\begin{aligned} \bar{G}_0(\boldsymbol{x}; \boldsymbol{x}_0) = \sum_{m=0}^{\infty} \frac{\epsilon_m}{2\pi^2} \cos\, m(\varphi - \varphi_0) \\ \cdot \int_0^\infty \left[K_m(\lambda\rho_0) - \frac{K_m(\lambda a)}{I_m(\lambda a)} I_m(\lambda\rho_0)\right] \\ \cdot I_m(\lambda\rho) \cos\lambda(z - z_0)\, d\lambda, \qquad |z_0| > L, \end{aligned} \tag{19}$$

where $\epsilon_m = 2 - \delta_{0m}$ denotes Neumann factor, and $I_m(\cdot)$ and $K_m(\cdot)$, the modified Bessel functions of first and second kinds, respectively.

We can evaluate the potential field $\phi_0(\boldsymbol{x})$ with the following volume integration of the above Green function:

$$\begin{aligned} \phi_0(\boldsymbol{x}) &= \iiint_V d\boldsymbol{x}_0 G_0(\boldsymbol{x}; \boldsymbol{x_0}) \underset{0}{\mathrm{div}}\, (\boldsymbol{v} \times \boldsymbol{B}) \\ &= \iiint_V d\boldsymbol{x}_0 \left(\underset{0}{\mathrm{grad}}\, G_0(\boldsymbol{x}; \boldsymbol{x_0})\right) \cdot (\boldsymbol{v} \times \boldsymbol{B}) \\ &= \iiint_V d\boldsymbol{x}_0 \big(\boldsymbol{B} \times \underset{0}{\mathrm{grad}}\, G_0(\boldsymbol{x}; \boldsymbol{x_0})\big) \cdot \boldsymbol{v}. \end{aligned} \tag{20}$$

Then, the flow signal is obtained as follows:

$$U_{\rm v} = \phi_0(a,0,0) - \phi_0(a,\pi,0). \tag{21}$$

Through the linearity of the integration (20), we define the differences of the Green funcutions at the points of signal pickup electrodes in the integrand as,

$$\begin{aligned}\boldsymbol{g}_0 \triangleq & \operatorname*{grad}_0 G_0(a,0,0;\rho_0,\phi_0,z_0) \\ & - \operatorname*{grad}_0 G_0(a,\pi,0;\rho_0,\phi_0,z_0),\end{aligned} \tag{22}$$

and

$$\begin{aligned}\bar{\boldsymbol{g}}_0 \triangleq & \operatorname*{grad}_0 \bar{G}_0(a,0,0;\rho_0,\phi_0,z_0) \\ & - \operatorname*{grad}_0 \bar{G}_0(a,\pi,0;\rho_0,\phi_0,z_0).\end{aligned} \tag{23}$$

These are considered the extensions of the virtual current distributions. Accordingly, the flow signal can be described as the following seperate volume integration:

$$\begin{aligned}U_{\rm v} = & \int_0^L dz_0 \int_0^a d\rho_0 \int_{-\pi}^{\pi} \rho_0\, d\varphi_0\, [\boldsymbol{B}\times\boldsymbol{g}_0]\cdot\boldsymbol{v} \\ & + \int_L^\infty dz_0 \int_0^a d\rho_0 \int_{-\pi}^{\pi} \rho_0\, d\varphi_0\, [\boldsymbol{B}\times\bar{\boldsymbol{g}}_0]\cdot\boldsymbol{v}.\end{aligned} \tag{24}$$

If $\boldsymbol{g}_0$ is used for the whole volume integral, we have the standard output signal; that is, the term $\boldsymbol{B}\times\boldsymbol{g}_0$ coincides with Bevir's original weight vector. Hence, in order to evaluate the end shorting effect, we focus the differnce of $\boldsymbol{g}_0$ to $\bar{\boldsymbol{g}}_0$ in the region of conducting pipe lines, $|z| > L$. Since the end-shorting effect comes from this region, we can evaluate it through the difference. Then, we integrate them to analyze end-shorting effect.

$$\delta U = \int_L^\infty dz_0 \int_{-\pi}^{\pi} \rho_0\, d\varphi_0 \int_0^a d\rho_0 [\boldsymbol{B}\times(\boldsymbol{g}_0 - \bar{\boldsymbol{g}}_0)]\cdot\boldsymbol{v}. \tag{25}$$

This evaluation of the end-shorting effect shows no dependence on liquid conductivity, which has been already expected from the problem formulation in this section. In order to analyze the effect of liquid conductivity on end-shorting, finite conductivity of the pipe line wall is taken into account in the next section.

4. FORMULATION & SOLUTION OF WALL POTENTIAL PROBLEM

Let us consider the pipe line with inner and outer radius of a and b respectively. We analyze the potential distribution over the pipe as shown in Fig.1.

Let the electric potential inside the fluid be $\phi_1(\rho,\varphi,z)$, and the one inside the pipe wall, $\phi_2(\rho,\varphi,z)$. If we let σ_1 and σ_2 be electrical conductivities of the fluid and the pipe wall, the potential problem is formulated as follows.

$$\Delta\phi_2 = 0, \qquad a<\rho<b, \tag{26}$$

$$\Delta\phi_1 = \operatorname{div}(\boldsymbol{v}\times\boldsymbol{B}), \qquad \rho<a, \tag{27}$$

$$\left.\frac{\partial\phi_2}{\partial\rho}\right|_{\rho=b} = 0, \tag{28}$$

$$\phi_1 = \phi_2 - \sigma_2\tau \left.\frac{\partial\phi_2}{\partial\rho}\right|_{\rho=a}, \qquad |z|>L$$

$$\sigma_1 \left.\frac{\partial\phi_1}{\partial\rho}\right|_{\rho=a} = \sigma_2 \left.\frac{\partial\phi_2}{\partial\rho}\right|_{\rho=a}, \qquad |z|>L \tag{29}$$

$$\left.\frac{\partial\phi_1}{\partial\rho}\right|_{\rho=a} = 0, \qquad |z|\le L. \tag{30}$$

In order to solve the problem, we introduce the corresponding Green functions, $G_1(\boldsymbol{x};\boldsymbol{x}_0)$ and $G_2(\boldsymbol{x};\boldsymbol{x}_0)$, as follows,

$$\Delta G_i(\boldsymbol{x};\boldsymbol{x}_0) = -\delta(\boldsymbol{x}-\boldsymbol{x}_0), \qquad i=1,2 \tag{31}$$

$$\left.\frac{\partial G_1}{\partial\rho_0}\right|_{\rho_0=a} = 0, \qquad |z_0|\le L \tag{32}$$

$$\sigma_1 \left.\frac{\partial G_1}{\partial\rho_0}\right|_{\rho_0=a} = \sigma_2 \left.\frac{\partial G_2}{\partial\rho_0}\right|_{\rho_0=a}, \qquad |z_0|>L \tag{33}$$

$$\left.\frac{\partial G_2}{\partial\rho_0}\right|_{\rho_0=b} = 0, \tag{34}$$

Since the meter region, $|z_0|\le L$, has the same Green function as (18) for G_1, we consider the pipe line region, $|z_0| > L$. The following Green functions are general solutions to the above potential problem in the pipe-line region.

$$\begin{aligned}G_1(\boldsymbol{x};\boldsymbol{x}_0) = & \sum_{m=0}^{\infty} \frac{\epsilon_m}{2\pi^2}\cos\, m(\varphi-\varphi_0) \\ & \cdot \int_0^\infty [K_m(\lambda\rho_0) + f_m(\lambda) I_m(\lambda\rho_0)] \\ & \cdot I_m(\lambda\rho)\cos\lambda(z-z_0)\, d\lambda,\end{aligned} \tag{35}$$

$$\begin{aligned}G_2(\boldsymbol{x};\boldsymbol{x}_0) = & \sum_{m=0}^{\infty} \frac{\epsilon_m}{2\pi^2}\cos\, m(\varphi-\varphi_0) \\ & \cdot \int_0^\infty [(K_m(\lambda\rho_0) + c_m(\lambda) I_m(\lambda\rho_0)) \\ & \qquad + d_m(\lambda) K_m(\lambda\rho_0) K_m(\lambda\rho)] \\ & \cdot \cos\lambda(z-z_0)\, d\lambda.\end{aligned} \tag{36}$$

From the boundary conditions, (32),(33) and (34), for the Green functions, we obtain the following relationship among expansion coefficients functions corresponding to

each $I_m(\lambda\rho)$, since (35) and (36) are series and integral expansions with a set of eigen functions.

$$c_m(\lambda) = -\frac{K'_m(\lambda b)}{I'_m(\lambda b)}, \tag{37}$$

$$d_m(\lambda) = 0, \tag{38}$$

$$f_m(\lambda) = (\sigma - 1)\frac{K'_m(\lambda a)}{I'_m(\lambda a)} - \frac{K'_m(\lambda b)}{I'_m(\lambda b)}, \tag{39}$$

$$\sigma \triangleq \frac{\sigma_2}{\sigma_1}. \tag{40}$$

Substituting these coefficient functions, $f_m(\lambda)$ and $c_m(\lambda)$, into (35) and (36) respectively, we obtain the following Green functions as a set of solutions:

$$\begin{aligned} G_1(\boldsymbol{x};\boldsymbol{x}_0) = &\sum_{m=0}^{\infty} \frac{\epsilon_m}{2\pi^2}\cos\, m(\varphi-\varphi_0) \\ &\cdot \int_0^{\infty} [K_m(\lambda\rho_0) \\ &+ \left((\sigma-1)\frac{K'_m(\lambda a)}{I'_m(\lambda a)} - \frac{K'_m(\lambda b)}{I'_m(\lambda b)}\right) I_m(\lambda\rho_0)\Big] \\ &\cdot I_m(\lambda\rho)\cos\lambda(z-z_0)\,d\lambda, \end{aligned} \tag{41}$$

$$\begin{aligned} G_2(\boldsymbol{x};\boldsymbol{x}_0) = &\sum_{m=0}^{\infty} \frac{\epsilon_m}{2\pi^2}\cos\, m(\varphi-\varphi_0) \\ &\cdot \int_0^{\infty} \left[(K_m(\lambda\rho_0) - \frac{K'_m(\lambda b)}{I'_m(\lambda b)} I_m(\lambda\rho_0)\right] \\ &\cdot I_m(\lambda a)\cos\lambda(z-z_0)\,d\lambda. \end{aligned} \tag{42}$$

The potential, $\phi_1(\boldsymbol{x})$, in the inner pipe can be evaluated by the same volume integration as (20),

$$\begin{aligned} \phi_1(\boldsymbol{x}) &= \iiint_V d\boldsymbol{x}_0 G_1(\boldsymbol{x};\boldsymbol{x_0}) \operatorname*{div}_0 (\boldsymbol{v}\times\boldsymbol{B}) \\ &= \iiint_V d\boldsymbol{x}_0 [\boldsymbol{B}\times \operatorname*{grad}_0 G_1(\boldsymbol{x};\boldsymbol{x_0})]\cdot\boldsymbol{v}. \end{aligned} \tag{43}$$

and we have the following flow signal,

$$U_{\mathrm{v}} = \phi_1(a,0,0) - \phi_1(a,\pi,0). \tag{44}$$

We define $\boldsymbol{g}_1$ and $\bar{\boldsymbol{g}}_1$ according to (22) and (23) in the previous section, and change the order of gradient operation as follows,

$$\begin{aligned} \boldsymbol{g}_1 &\triangleq \operatorname*{grad}_0 G_1(a,0,0;\rho_0,\phi_0,z_0) \\ &\quad - \operatorname*{grad}_0 G_1(a,\pi,0;\rho_0,\phi_0,z_0) \\ &= \operatorname*{grad}_0 \sum_{m:\mathrm{odd}} \frac{2}{\pi^2}\cos\, m\varphi_0 \\ &\quad \int_0^{\infty} \left(K_m(\lambda\rho_0) - \frac{K'_m(\lambda a)}{I'_m(\lambda a)} I_m(\lambda\rho_0)\right) \\ &\quad \cdot I_m(\lambda a)\cos\lambda z\; d\lambda, \end{aligned} \tag{45}$$

$$\begin{aligned} \bar{\boldsymbol{g}}_1 &\triangleq \operatorname*{grad}_0 \bar{G}_1(a,0,0;\rho_0,\phi_0,z_0) \\ &\quad - \operatorname*{grad}_0 \bar{G}_1(a,\pi,0;\rho_0,\phi_0,z_0) \\ &= \operatorname*{grad}_0 \sum_{m:\mathrm{odd}} \frac{2}{\pi^2}\cos\, m\varphi_0 \\ &\quad \cdot \int_0^{\infty} \Big[K_m(\lambda\rho_0) + \Big((\sigma-1)\frac{K'_m(\lambda a)}{I'_m(\lambda a)} \\ &\quad - \frac{K'_m(\lambda b)}{I'_m(\lambda b)}\Big) I_m(\lambda\rho_0)\Big] I_m(\lambda a)\cos\lambda z\, d\lambda. \end{aligned} \tag{46}$$

Again, the effect of end shorting is evaluated by the difference between them, that is,

$$\begin{aligned} \boldsymbol{g}_1 - \bar{\boldsymbol{g}}_1 = \operatorname*{grad}_0 &\sum_{m:\mathrm{odd}} \frac{2}{\pi^2}\cos\, m\varphi_0 \\ &\int_0^{\infty} \left(-\sigma\frac{K'_m(\lambda a)}{I'_m(\lambda a)} + \frac{K'_m(\lambda b)}{I'_m(\lambda b)}\right) \\ &I_m(\lambda\rho_0) I_m(\lambda a)\cos\lambda z_0\, d\lambda \end{aligned} \tag{47}$$

The elements of this difference vector read,

$$\begin{aligned} (\boldsymbol{g}_1 - \bar{\boldsymbol{g}}_1)_\rho = &\sum_{m:\mathrm{odd}} \frac{2}{\pi^2}\cos m\varphi_0 \\ &\cdot \int_0^{\infty} \left(-\sigma\frac{K'_m(\lambda a)}{I'_m(\lambda a)} + \frac{K'_m(\lambda b)}{I'_m(\lambda b)}\right) \\ &\cdot \lambda I'_m(\lambda\rho_0) I_m(\lambda a)\cos\lambda z_0\, d\lambda \end{aligned} \tag{48}$$

$$\begin{aligned} (\boldsymbol{g}_1 - \bar{\boldsymbol{g}}_1)_\varphi = -&\sum_{m:\mathrm{odd}} \frac{2}{\pi^2} m\sin m\varphi_0 \\ &\cdot \int_0^{\infty} \left(-\sigma\frac{K'_m(\lambda a)}{I'_m(\lambda a)} + \frac{K'_m(\lambda b)}{I'_m(\lambda b)}\right) \\ &\cdot \frac{1}{\rho_0} I_m(\lambda\rho_0) I_m(\lambda a)\cos\lambda z_0\; d\lambda, \end{aligned} \tag{49}$$

$$\begin{aligned} (\boldsymbol{g}_1 - \bar{\boldsymbol{g}}_1)_z = -&\sum_{m:\mathrm{odd}} \frac{2}{\pi^2}\cos m\varphi_0 \\ &\cdot \int_0^{\infty} \left(-\sigma\frac{K'_m(\lambda a)}{I'_m(\lambda a)} + \frac{K'_m(\lambda b)}{I'_m(\lambda b)}\right) \\ &\cdot \lambda I_m(\lambda\rho_0) I_m(\lambda a)\sin\lambda z_0\; d\lambda. \end{aligned} \tag{50}$$

Before detailed evaluations, we consider the simplified case same as in [5]. Let us suppose the uniform magnetic

field along y-axis in cylindrical coordinates and not a fully developed but uniform flow profile, as follows,

$$\boldsymbol{B} = [B\sin\varphi, B\cos\varphi, 0]^{\mathsf{T}} \tag{51}$$

$$\boldsymbol{v} = [0, 0, v_0]^{\mathsf{T}} \tag{52}$$

Then, the end-short effect δU is evaluated through the orthogonality of the eigenfunctions, $\sin, \cos, I_m, K_m$, by change the order of integrations. Since the magnetic field is uniform, orthgonality of trigonometric functions admits $m = 1$ only. After the evaluation of the each integration, we have the following estimate,

$$\begin{aligned}
\delta U &= \int_L^\infty dz_0 \int_{-\pi}^{\pi} \rho_0\, d\varphi_0 \int_0^a d\rho_0 [\boldsymbol{B} \times (\boldsymbol{g}_1 - \bar{\boldsymbol{g}}_1)] \cdot \boldsymbol{v} \\
&= \int_L^\infty dz_0 \int_{-\pi}^{\pi} \rho_0\, d\varphi_0 \int_0^a d\rho_0 [\boldsymbol{B} \times (\boldsymbol{g}_1 - \bar{\boldsymbol{g}}_1)]_z v_0 \\
&= \frac{2Bv_0}{\pi} \int_L^\infty dz_0 \int_0^a d\rho_0 \int_0^\infty \left(\sigma \frac{K_1'(\lambda a)}{I_1'(\lambda a)} - \frac{K_1'(\lambda b)}{I_1'(\lambda b)} \right) \\
&\qquad (I_1(\lambda\rho_0) + \lambda\rho_0 I_1'(\lambda\rho_0))\, I_1(\lambda a) \cos\lambda z_0\, d\lambda.
\end{aligned} \tag{53}$$

Integration with respect to z_0 is evaluated as,

$$\begin{aligned}
\int_L^\infty \cos\lambda z_0\, dz_0 &= \int_0^\infty \cos\lambda z_0\, dz_0 - \int_0^L \cos\lambda z_0\, dz_0 \\
&= \frac{1}{2}\delta(\lambda) - \frac{\sin\lambda L}{\lambda},
\end{aligned} \tag{54}$$

and that with respect to ρ_0,

$$\begin{aligned}
\int_0^a (I_1(\lambda\rho_0) + \lambda\rho_0 I_1'(\lambda\rho_0))\, d\rho_0 &= \Big[\rho_0 I_1(\lambda\rho_0)\Big]_0^a \\
&= a I_1(\lambda a).
\end{aligned} \tag{55}$$

Finally we obain the following end shorting effect:

$$\begin{aligned}
\delta U = -\frac{2Bv_0 a}{\pi} \Bigg[&\frac{1}{8}\left(\sigma + \frac{a^2}{b^2}\right) \\
&+ \int_0^\infty \left(\sigma \frac{K_1'(\lambda a)}{I_1'(\lambda a)} - \frac{K_1'(\lambda b)}{I_1'(\lambda b)} \right) \{I_1(\lambda a)\}^2 \frac{\sin\lambda L}{\lambda} d\lambda \Bigg]
\end{aligned} \tag{56}$$

This effect converges to 0 as the meter length of L and the area of exciting magnetic field approach infinity. If the pipe line conductivety is sufficiently high, namely, $\sigma \gg 1$, it approaches to the equation (25), since $K_1'(\lambda b)/I_1'(\lambda b)$ is negative and integration is canceled with $\sigma/4$. This evaluation gives the supreme effect, since the magnetic field and the velocity profile have the distributions,

Figure 2 shows experimantal results given in the Japanese patent[3], and exhibits the agreement with (56) in spite of violation of the uniformity assumption.

5. CONCLUSIONS

We have derived the presice formula to evaluate end-shorting effects on electromagnetic flowmeters. Practical evaluation needs numerical treatments based on theoretical analyses.

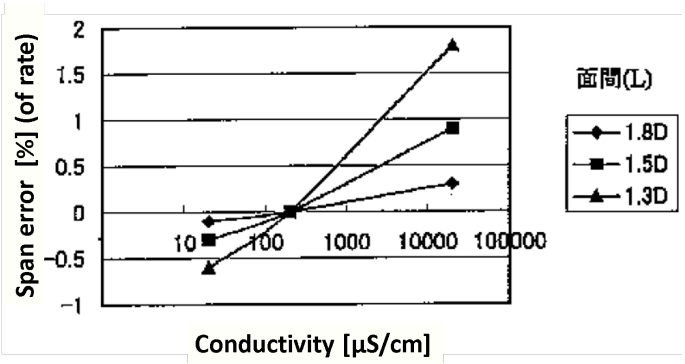

Fig. 2. Span errors for various conductivity fluid[3].

REFERENCES

[1] J.A.Shercliff, The Theory of Electromagnetic Flow-Measurement, Cambridge University Press, 1962.

[2] G.Schmmartz, Induktive Strömungsmessung, VEB Verlag Technik, 1974.

[3] T.Arai, Japan Patent Kokai 2002-310750 (2002.10.23)

[4] M.K.Bevir, Induced Voltage Electromagnetic Flowmeters, Journal of Fluid Meachanics, Vol. 43, part 3, pp. 577–590, 1971.

[5] M.K.Bevir, The effect of conducting pipe connections and surrounding liquid on the sensitivity of electromagnetic flowmeters, J.Phys. D: Appl.Phys., Vol. 5, pp. 717–729, 1972.

[6] M.K.Bevir, V.T.O'Sullivan and D.G.Wyatt, Computation of electromagnetic flowmeter characteristics from magnetic filed data, J.Phys. D: Appl.Phys., Vol. 14, pp. 373–368, 1981.

[7] D.G.Wyatt, Computation of electromagnetic flowmeter characteristics from magnetic field data:II. Errors, J.Phys. D: Appl.Phys., Vol. 16, pp. 465–478, 1983.

[8] J.Hemp and H.K.Versteeg, Prediction of electromagnetic flowmeter characteristics, J.Phys. D: Appl.Phys., Vol. 19, pp. 465–478, 1983.

[9] S.Honda, End-shorting Effect on Electromagnetic Flowmeters, Proc. FLOMEKO 2014, Paris, 2014.

[10] S.Honda and T.Yamamoto A New Configuration of Electro-Magnetic Flowmeters with Self-Calibration — Theoretical Analysis, Proc. SICE ANNUAL CONFERENCE 2004, IEEE Xplorer, 2004.

[11] S.honda, Recent Advances in Electromagnetic Flowmeters: Does Is Measure only Average Flowrate?, Proc.FLUCOME 2007 Tallahassee, 2007.

[12] V.Cushing, Induction Flowmeter, Review of Scientific Instrument, Vol. 29, No. 8, pp. 692–697, 1958.